Sodium Chloride, NaCl/ε: New Force Field

Raúl Fuentes-Azcatl* and Marcia C. Barbosa*

Instituto de Física, Universidade Federal do Rio Grande do Sul, Caixa Postal 15051, CEP 91501-970 Porto Alegre, Rio Grande do Sul, Brazil

ABSTRACT: A new computational model for sodium chloride, the NaCl/ε, is proposed. The force field employed for the description of the NaCl is based on a set of radial particle–particle pair potentials involving Lennard-Jones (LJ) and Coulombic forces. The parametrization is obtained by fitting the density of the crystal and the density and the dielectric constant of the mixture of the salt with water at a diluted solution. Our model shows good agreement with the experimental values for the density and for the surface tension of the pure system, and for the density, the viscosity, the diffusion, and the dielectric constant for the mixture with water at various molal concentrations. The NaCl/ε together with the water TIP4P/ε models provide a good approximation for studying electrolyte solutions.
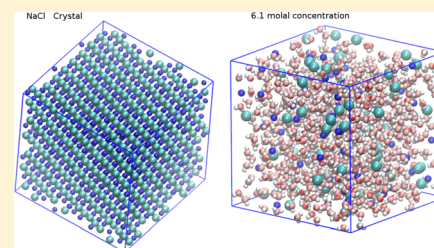
1. INTRODUCTION

Sodium chloride is present in our lives from the chemical balance of our body to the geophysical and biological equilibrium of the planet. It is also largely used in industry, particularly to preserve food. Therefore, the understanding of physical–chemical properties of sodium chloride as a pure substance or in mixtures is important. One of the key questions regarding salt is how it behaves in solution under different pressures and temperatures and also under confinement.[1–4]

A number of experimental studies have addressed the behavior of sodium chloride in water.[5,6] Even though they provide the behavior of the thermodynamic and of the dynamic quantities as a function of temperature and pressure, due to the high number of variables that influence these properties, it becomes difficult to identify which is the mechanism behind the behavior of the salt solutions. Then, the theoretical methods become a complementary tool that not only allows for exploring a wider range of parameters but also provides a more controlled analysis of the parameters. Due to the long-range nature of the Coulomb interactions, analytic approaches for describing the behavior of the ions, Na^+ and Cl^-, in water require approximations that either limit the analysis to very low dilution[7] or to the study of systems far from phase separations.[8] Consequently, after the development of approaches to account for the electrostatic interactions,[9,10] simulations became an important strategy to study electrolyte solutions.

The crucial step in the simulations is to construct an appropriate force field for the interaction potential between the ions and the water. The usual method is to fit the parameters of the model with the experimental results for the density and for the structure for the real system at one determined pressure and temperature. Then, the results obtained for thermodynamic and dynamic properties with the model are compared with those from experiments. Following this procedure, a number of models for sodium chloride[11] capable of reproducing the density of the pure system have been developed.

Recently, Smith et al.[11] studied 13 of the most common NaCl force fields. These models, even though they reproduce some of the properties of the crystal, are unable to capture others. For instance, just one of them reproduced the correct density, and other obtained the correct chemical potential of the solid phase at room temperature. In parallel to modeling the salt, numerical strategies have been employed to build computational models for water.[12–15] These models reproduce the density of water around 298 K and a pressure of 1 bar[16] but fail to provide a reliable value for a number of properties, including the dielectric constant.[17]

In the case of studying electrolyte solutions, the common strategy is to combine one model for water and one model for salt that have been obtained by fitting the properties of the pure systems. Then, the mixture of these two models is tested. The solubility is one of the main properties used to validate the model of salt. When dissolved in water, the molecule of sodium chloride dissociates in one cation, Na^+, and one anion, Cl^-. Due to the polar character of the water molecules both ions become surrounded by water molecules.[5] For certain salt concentrations the system phase separates in a salt rich phase and salt poor phase. The solubility can be computed in this coexistence.

One method for computing the coexistence between the crystal and the saturated phase is to estimate the chemical potentials independently.[18,19] For the solid, the absolute free energy of the crystal can be computed using the method proposed by Frenkel and Ladd.[20] Employing this framework, Sanz and Vega[19] determined the solubility of KF and NaCl in the water solution. This procedure was also employed for a variety of salts in water[21–23] for computing not only the solubility but also other properties of the salt solution.[24,25] Within the same method, the best comparison between the

experimental values for the solubility and the simulations was computed by Smith and co-workers.[11]

Another approach to obtain the salt rich and salt poor coexistence is to use a sufficiently large crystal in contact with an almost saturated ion solution.[26] The main assumption is that this crystal and the solution reach an equilibrium state after very long simulations and extremely large systems; otherwise, finite size effects dominate.[27]

The drawback of analyzing the water and salt mixture using the NaCl and water models parametrized for the pure systems is that, when mixed, the water surrounds the ions, affecting the salt−salt and water−water interactions. In this work we present a new model for NaCl that is parametrized to reproduce properties of the pure salt and of the water−salt mixture. The behavior of the model is tested against experiments for properties of the pure salt and of the water−salt solution. In the salt−water mixture, two water models designed to give the correct dielectric constant of water were employed: the SPC/ϵ[28] and the TIP4P/ϵ.[17] For computing the solubility we follow the Manzanilla et al.[27] approach with the crystal surrounded by the saturated solution to avoid finite size effects.

The remainder of the paper goes as follows. In section 2, the new model for NaCl is introduced, and the two water models employed for the parametrization of the salt were reviewed. Section 3 summarizes the simulation details, and the results are analyzed in section 4. The conclusions are presented in section 5.

2. MODELS

NaCl/ϵ Model. The force field employed here for the description of the NaCl in the aqueous solution is based on a set of radial particle−particle pair potentials involving Lennard-Jones (LJ) and Coulombic contributions, namely

$$u(r_{ij}) = 4\xi_{ij}\left[\left(\frac{\sigma_{ij}}{r_{ij}}\right)^{12} - \left(\frac{\sigma_{ij}}{r_{ij}}\right)^{6}\right] + \lambda_i\lambda_j\frac{q_iq_j}{4\pi\epsilon_0 r_{ij}}$$

(1)

where r_{ij} is the distance between sites i and j, q_i is the electric charge of site i, ϵ_0 is the permittivity of vacuum, ξ_{ij} is the potential depth, and σ_{ij} is the distance at which the interparticle potential is zero.

We assume that the pure water and the ion potentials are compatible. This means that the cross interactions between the water molecules and the ions can be calculated by the Lorentz−Berteloth (LB) combining rules for the conformal LJ potential[29]

$$\sigma_{\alpha\beta} = \left(\frac{\sigma_{\alpha\alpha} + \sigma_{\beta\beta}}{2}\right) \qquad \xi_{\alpha\beta} = \sqrt{\xi_{\alpha\alpha}\xi_{\beta\beta}}$$

(2)

For the NaCl/ϵ model the NaCl is considered an ion pair, $\xi_{ij} = \xi_{LJ}$, while $\sigma_{ij} = \sigma_{LJ}$ for any i and j, namely, for Na−Na, Cl−Cl, or Na−Cl.[30] The spherical anions and cations are represented by a single interactive site at their centers, carrying charges $q_i = \pm 1e$ where e is the charge of an electron. In order to correct for the nonpolarizability of the model, the Coulombic term is corrected by a screening factor $\lambda_i = \lambda_C$ for both sodium and chloride ions. This factor is used both in the pure salt system and in the solution with water. Therefore, there are three parameters, namely, λ_C, σ_{LJ}, and ξ_{LJ} to be adjusted with experimental data for each ion. The assumption that polarizable models for some temperature and pressures can be reduced to simple nonpolarizable models was introduced by Leontyev and

Stuchebrukhov[31] for the particular case of ionic liquids. Here we explore this idea for the screening of the salt ions.

The parametrization process was made as follows. First, the parameters were selected so that the NaCl/ϵ force field reproduces the experimental value for the density of the crystal in the face centered cubic phase at 1 bar and 298 K.[5,32] There are several parametrizations of the NaCl model that give the proper density value. A table with all these values, including the parameters used by other models, was made. Next, all the possibilities were checked with the radial distribution function, $g(r)$, and a subset of parameters which give the correct density and also describe the structure of the salt crystal at 1 bar and 298 K were selected. This step provided the first approximation for the parameters of the model.

Then, the parameters which give the density and the structure were tested for the density and the dielectric constant in the mixture of the salt with water[5] at 1 bar, 298 K, and 4 molal salt concentration. At this concentration the ions are hydrated, and there are no clusters starting a nucleation. Finally, the parameters for the NaCl/ϵ model found through this process are shown in Table 1.

Table 1. Force Field Parameter of NaCl/ϵ

model	q/e	λ_C	$\sigma/$Å	$(\xi/k_B)/$K
Na	+1	0.885	2.52	17.44
Cl	−1	0.885	3.85	192.45

TIP4P/ϵ Water Model. The TIP4P/ϵ[17] model defines the water molecule as rigid and nonpolarizable with the same geometry of the TIP4P as illustrated in Figure 1. The
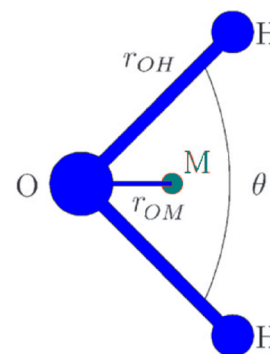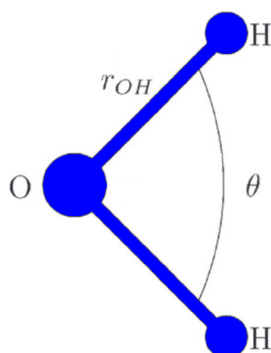

Figure 1. Schematic representation of the TIP4P water model. The distance between the oxygen and the hydrogen is r_{OH}, and the angle between the oxygen and the two hydrogens is θ. The hydrogens have positive charge while the negative charge is located at a point M that is r_{OM} distant from the oxygen that contains no charge.

intermolecular force field between two water molecules is given by the Lennard-Jones and the Coulomb interactions as given by eq 1. The TIP4P models have a positive charge at each hydrogen and a negative charge along the bisector of the HOH angle located at a distance l_{OM} of the oxygen as shown in Figure 1. The geometry and parameters of the force fields for the TIP4P/ϵ are given in Table 2. In the case of the TIP4P/ϵ model, $\lambda_O = \lambda_H = 1$ in eq 1.

SPC/ϵ Model. The SPC/ϵ is another model for water. It is based on the SPC model geometry shown in Figure 2, but with a different set of parameters. The SPC/ϵ model[28] defines water as rigid and nonpolarizable as illustrated in Figure 2. The

Table 2. Force Field Parameters of TIP4P/ϵ Water Model[a]

model	$r_{OH}/Å$	Θ/deg	q_H/e	q_M/e	$r_{OM}/Å$	$\sigma/Å$	$(\xi/k_B)/K$
TIP4P/ϵ	0.9572	104.52	0.527	1.054	0.105	3.165	93

[a]The charge in site M is $q_M = -(2q_H)$.

Figure 2. Schematic representation of the SPC water model. The distance between the oxygen and the hydrogen is r_{OH}, and the angle between the oxygen and the two hydrogens is θ. The hydrogens have positive charge while the oxygen carries the negative charge.

intermolecular force field between two water molecules is given by the Lennard-Jones and the Coulomb interactions as given by eq 1 with $\lambda_O = \lambda_H = 1$. The parametrization was made using the dipole moment of the minimum density method μ_{md}.[17]

The SPC/ϵ model gives similar thermodynamic and dynamic properties as the SPC[12] and the SPC/E[13] models, but better agreement with the experiments for the dielectric constant.[45]

The geometry and parameters of the force fields analyzed in this work are given in Table 3.

Table 3. Force Field Parameters of Water Model, SPC/ϵ[a]

model	$r_{OH}/Å$	Θ/deg	q_H/e	$\sigma/Å$	$(\xi/k_B)/K$
SPC/ϵ	1	109.45	0.445	3.1785	84.9

[a]The charge of oxygen is $q_O = -(2q_H)$.

3. SIMULATION DETAILS

Molecular dynamic (MD) simulations were performed using GROMACS[33] (version 4.5.5.). The equations of motion were solved using the leapfrog algorithm,[10,33] and the time step was 2 fs; the time of simulations of different molalities is 30 ns, keeping the positions and velocities for every 500 steps in simulation. The calculus of the shear viscosity, however, employed 1 fs, the time of simulations is 40 ns, storing the positions and velocities every simulation step. Ewald summations were used to deal with electrostatic contributions. The real part of the Coulombic potential is truncated at 10 Å. The Fourier component of the Ewald sums was evaluated by using the smooth particle mesh Ewald (SPME) method[34] using a grid spacing of 1.2 Å and a fourth degree polynomial for the interpolation. The simulation box is cubic throughout the whole simulation and the geometry of the water molecules kept constant using the LINCS procedure.[35] Temperature has been set to the desired value with a Nosé−Hoover thermostat.[36] The pressure is obtained using the Parinell−Rahman barostat with a τ_P parameter of 1.0 ps.[33]

The MD simulations of pure NaCl made in the NPT ensemble were carried out under 1 bar pressure condition, on a system of 1024 NaCl pairs, with a time step $\Delta t = 2$ fs; the time of simulations is 10 ns with storing the positions and velocities every 1000 simulation step. The coexisting liquid and vapor phases of NaCl were analyzed in the NVT ensemble on a system of 2916 NaCl pairs in an elongated simulation cell of dimensions $L_x = L_y = 3L_z$; the time of simulations is 10 ns with storing the positions and velocities every 500 simulation step and using $r_{cut} = 2.6$ nm. The densities of the two phases were extracted from the statistical averages of the liquid and vapor limits of the density profiles.[37] The corresponding surface tension γ of one planar interface was calculated from the mechanical definition of γ[38]

$$\gamma = 0.5L_z[P_{zz}0.5P_{xx} + P_{yy}] \tag{3}$$

where $P_{\alpha\alpha}$ are the diagonal elements of the microscopic pressure tensor. The factor 0.5 outside the squared brackets takes into account the two symmetrical interfaces in the system.

For sodium chloride, NaCl/ϵ in water, the simulations have been done using 864 molecules in the isothermal−isobaric ensemble NPT, in liquid phase at different molalities and a temperature of 298 K and 1 bar of pressure. The molality concentration is obtained from the total number of ions in solution N_{ions}, the number of water molecules N_{H_2O}, and the molar mass of water M_{H_2O} as

$$[NaCl] = \frac{N_{ions} \times 10^3}{2N_{H_2O}M_{H_2O}} \tag{4}$$

The division by 2 in this equation accounts for a pair of ions, and $M_{H_2O} = 18$ g mol^{-1}. Table 4 gives the value of the molality for each point of calculus.

Table 4. Composition of NaCl Solutions Used in the Simulations at 298.15 K and 1 bar

molality (m)	N_{H_2O}	N_{ions}
0.06	862	2
0.99	832	32
1.99	806	58
3.07	778	86
4.05	754	110
5.0	732	132
5.93	712	144
6.02	710	154
6.31	704	160

The static dielectric constant is computed from the fluctuations[39] of the total dipole moment **M**

$$\epsilon = 1 + \frac{4\pi}{3k_BTV}(\langle \mathbf{M}^2 \rangle - \langle \mathbf{M} \rangle^2) \tag{5}$$

where k_B is the Boltzmann constant and T the absolute temperature. The dielectric constant is obtained for long simulations at constant density and temperature or at constant temperature and pressure. The shear viscosity is obtained using the autocorrelation function of the off-diagonal components of

the pressure tensor $P_{\alpha\beta}$ according to the Green–Kubo formulation

$$\eta = \frac{V}{k_B T} \int_0^\infty \left\langle P_{\alpha\beta}(t_0) P_{\alpha\beta}(t_0 + t) \right\rangle_{t_0} dt \tag{6}$$

The self-diffusion coefficient, D, is obtained from the Einstein equation

$$D = \lim_{t \to \infty} \frac{1}{6t} \langle |\mathbf{R}_i(t) - \mathbf{R}_i(0)|^2 \rangle \tag{7}$$

where $\mathbf{R}_i(t)$ is the center of mass position of molecule i at time t and $\langle ... \rangle$ denotes time average.

Even thought the thermodynamic and dynamic quantities were produced for 864 number of particles for each density, systems with 1024 and 2048 were also tested showing a difference in the result smaller than the data points used in the plots. For the solubility computations, where the errors are larger, 2048 particles were employed. In this particular case the error bars are on the order of 2.7% of the computed values.

4. RESULTS

Pure Sodium Chloride NaCl/ϵ. The pure NaCl is analyzed. First, the parameters for the model were fitted to give the experimental value for the density of the NaCl crystal at the temperature of $T = 298$ K and at the pressure of 1 atm, namely, 2.16 g cm^{-3}.[5] Within the parameter values which produce this density, we select the subset that also gives the radial distribution for Na–Na, Cl–Cl, and Na–Cl as illustrated in Figure 3. This result shows a peak in the curve for the Na–Cl at 2.78 in agreement with the experiments.[5]
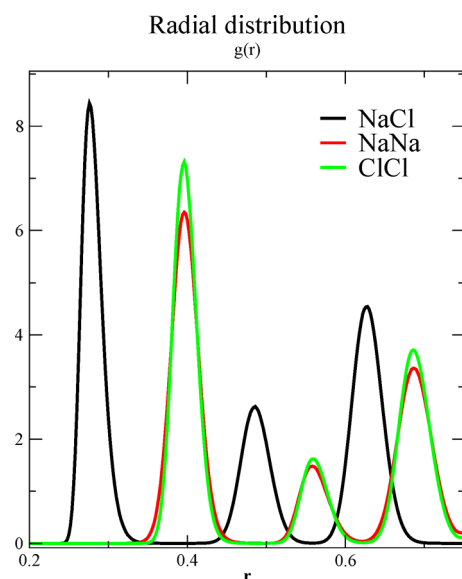

Figure 3. Radial distribution function $g(r)$ versus the distance r at 1 bar and 298 K for: Na–Na (red line), Cl–Cl (green line), and Na–Cl (black line).

Following this procedure the resulting lattice energy (LE) for the NaCl/ϵ model is 669.21 kJ/mol while the experimental data gives 790 kJ/mol.[5] The lattice constant (LC) for the same model is 5.56 while the experimental value is 5.64.[5]

The reason for the difference between the values for the lattice energy obtained within our approach and the experiments is due to the "screening" factor λ. In order to be consistent with the idea that the λ works for screening the lattice energy for the NaCl/ϵ model should be computed in a renormalized form what it will be explored in a future publication.

In order to validate our model, Table 5 shows the values for the density, the lattice energy, and the lattice constant for the

Table 5. Density of NaCl at Room Pressure and Temperature, Lattice Energy, and Lattice Constant of Various Force Fields and for Experiments[5]

model ions	$\rho/(\text{g/cm}^3)$	LC/Å	LE/(kcal/mol)
JJ[40]	1.78	5.9	796.26
JC$_{S3}$[32]	1.97	5.7	800.4
JC$_{T4}$[32]	2.05	5.78	792.88
ACB[38]	2.16	5.47	816.37
this work	2.16	5.56	669.21
exptl[5]	2.16	5.64	789.95

NaCl/ϵ in comparison with other force fields all at 1 bar of pressure and 298 K of temperature. While the Alejandre et al.[38] (ACB) gives good results for the density, the JJ[40] model and the two parametrizations of the JC[32] approach (JC$_{S3}$ and JC$_{T4}$) show good results for the lattice crystal and for the lattice energy when compared with the experimental results. Our model gives good agreement with the experiments[5] for the density of the crystal and for the lattice constant, but is a quite far from the reproduction of the lattice energy probably due to the way the lattice energy should be modified for the NaCl/ϵ as explained above.

Another important validation for the NaCl/ϵ is to check if the density of the liquid phase, for temperatures higher than the region from which the fitting was done, agrees with the experimental results. Figure 4 illustrates the isobar at 1 bar for the density versus temperature for the system both in the solid
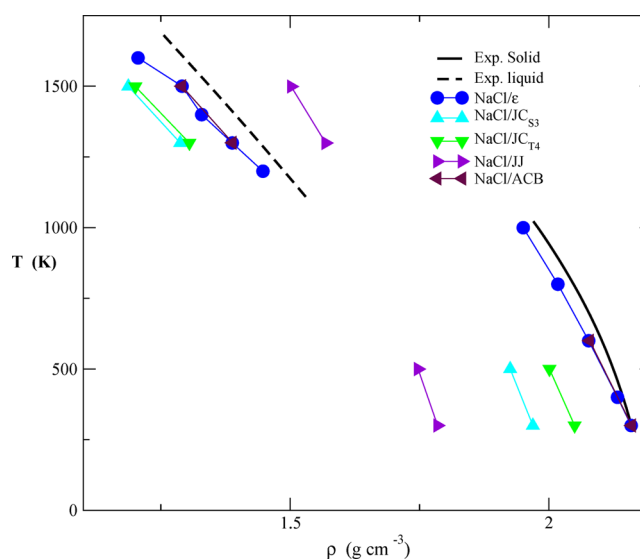

Figure 4. Temperature versus density of NaCl at the liquid ($T > 1000$ K) and solid ($T < 1100$ K) phases. The solid and dashed black lines are the experimental data,[5] and the blue filled circles are for the NaCl/ϵ model. The results for the ACB[38] model are represented by brown filled triangles, and those for the JJ[40] model are shown by purple filled triangles. Results for the JC$_{S3}$[32] model are shown by blue triangles, and those for the JC$_{T4}$ model are shown as green triangles.

and liquid phases. Our results for the pure NaCl/ϵ (solid circles) are compared with the experimental data (solid and dashed lines)[5] and with the results of Alejandre et al.[38] (ACB), the JJ[40] model, and the two parametrizations of the JC[32] (JC$_{S3}$ and JC$_{T4}$). The NaCl/ϵ shows a better agreement with the experiments than the other simulations.

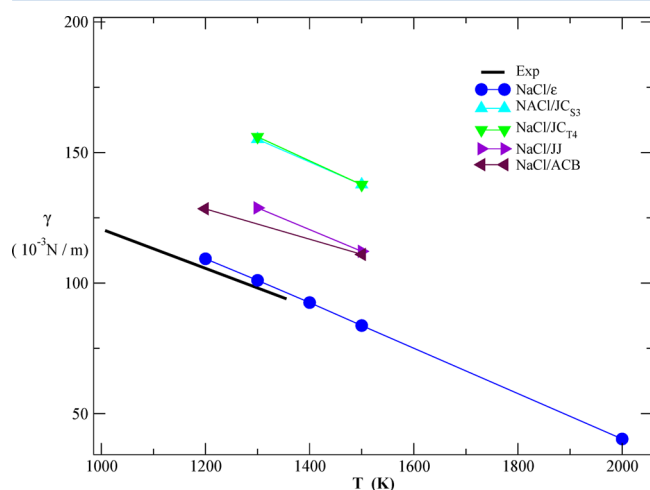In addition to the density, the surface tension was also computed. Figure 5 illustrates the temperature versus surface

Figure 5. Surface tension versus temperature for the pure NaCl system at 1 bar of pressure. The black line is the experimental data,[5] and the blue circles are for the NaCl/ϵ. The results for the ACB[38] model are represented by brown filled triangles, and those for the JJ[40] model are shown by purple filled triangles. Results for the JC$_{S3}$[32] model are shown by blue triangles, and those for the JC$_{T4}$ model are shown as green triangles.

tension for the NaCl/ϵ compared with the experiments and the other models. Our model shows a better agreement with the experimental surface tension when compared with the ACB,[38] JJ,[40] JC$_{S3}$,[32] and JC$_{T4}$[32] models.

Sodium Chloride NaCl/ϵ in the TIP4P/ϵ Water. The thermodynamic and dynamic properties of the NaCl/ϵ in solution with the TIP4P/ϵ water are checked against experimental results and other models. Figure 6 illustrates the dielectric constant versus salt molal concentrations at 298 K and 1 bar for the NaCl/ϵ in the TIP4P/ϵ water model (blue diamond) compared with the experimental data (solid black line),[5] with the JJ[40] salt model in the TIP4P/ϵ water (purple triangles) and in the TIP4P (dark blue triangles) water models, respectively. In the case of the JJ[40] salt model the simulations show phase separation for salt concentrations above 1 molar, so the dielectric constant was not computed. The figure also presents results for the JC$_{T4}$[32] model in the TIP4P/Ew water (dark green triangles) and in the TIP4P/ϵ water, respectively (light green triangles). Our results indicate that, even thought the parameters for the NaCl/ϵ model were fitted to give the experimental dielectric constant for the concentration 4 mol/kg (shown in the figure as a purple circle), the model in the TIP4P/ϵ water gives good agreement with the experiments over a wider range of molal concentrations.

Next, Figure 7 shows the density of the mixture of NaCl and water as a function of the salt molal concentration at 1 bar and 298 K for our model, other models, and the experimental results. Since most models are parametrized to give the correct
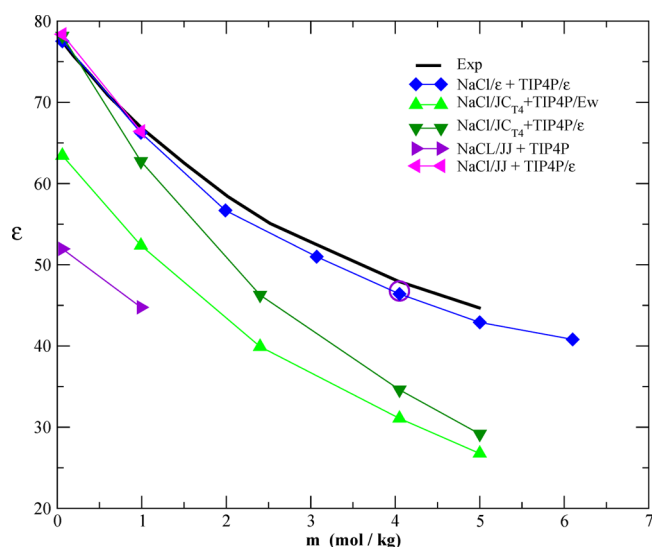

Figure 6. Dielectric constant of the mixture versus molal concentration of the salt at the temperature 298 K and at 1 bar of pressure. The black line is the experimental data,[5] and the blue filled diamond shows the results for the NaCl/ϵ. The violet circle is the concentration in which the parametrization of our model was made. The purple and the dark blue triangles are for the JJ salt model in the TIP4P/ϵ and in the TIP4P water models, respectively. The light and dark green triangles are for the JC$_{T4}$ salt model in the TIP4P/Ew and in the TIP4P/ϵ water models, respectively. All the simulations have been performed in this work.
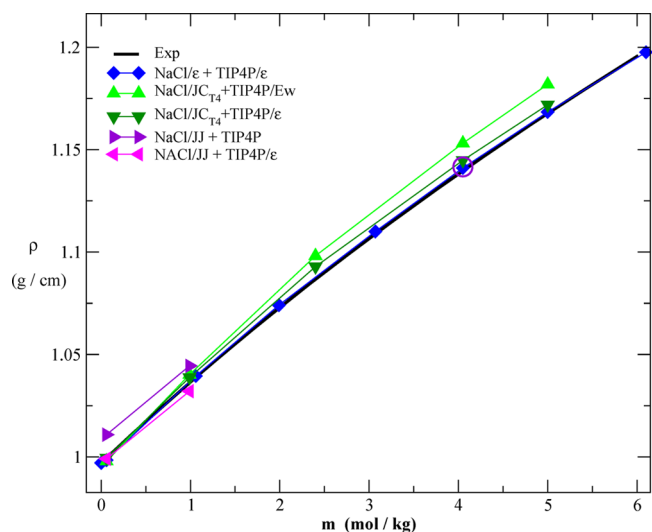

Figure 7. Density of the mixture versus molal concentration of the salt at the temperature of 298 K and at 1 bar pressure. The black line is the experimental data,[5] and the blue filled diamonds are the results for the NaCl/ϵ model. The violet circle is the diluted concentration where the parametrization was made. The purple and the dark blue triangles are for the JJ model in the TIP4P/ϵ and in the TIP4P water models, respectively. The light and dark green triangles are the results for the JC$_{T4}$ salt model in the TIP4P/Ew and in the TIP4P/ϵ water models, respectively.

experimental density, for all the models presented in this paper the agreement with the experiments are good.

Since our model introduces a new parameter related to the hydration of the ions, the structure of the water molecules around ions is computed and checked with experimental results. The hydration is measured by the four partial pair
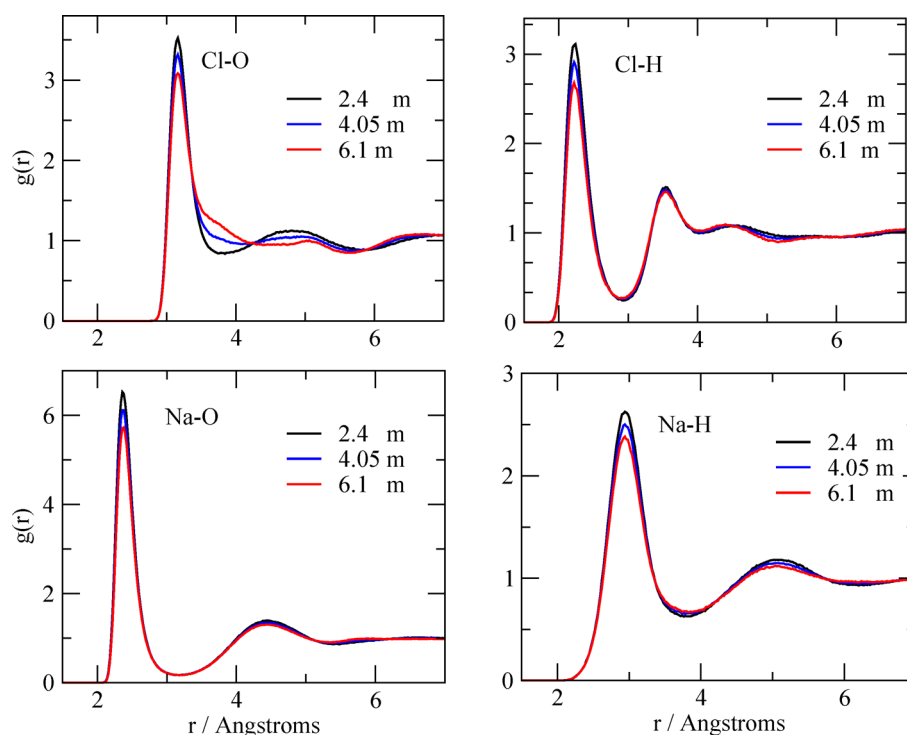
Figure 8. Ion−water pair distribution functions using the rigid water model TIP4P/ϵ and NaCl/ϵ force field at 298 K, 1 bar, and ionic concentrations of 2.4 (black line), 4.05 (blue line), and 6.1 (red line) molal. In all cases 864 molecules were used.

distribution functions g_{NaH}, g_{ClH}, g_{NaO}, and g_{ClO}.[38] The calculus of these functions with the TIP4P/ϵ and NaCl/ϵ force fields is shown in the Figure 8 for molal concentrations of 2.4, 4.05, and 6.1 molal. We can see that, as the salt is diluted in water, the structure is favored around each ion, as illustrated by the larger amplitudes of the first peaks, which points to a slightly stronger hydration. Having a smaller number of coordinating the anion has more mobility, as seen in the calculation of the diffusion coefficient.

The peak positions, r_{max}'s, of the pair distribution functions in our model are given by the following: $r_{max} \cong 3.0$ Å for Na−H, $r_{max} \cong 2.25$ and 3.55 Å for the first and second peaks of Cl−H, and $r_{max} \cong 2.37$ Å for Na−O and 3.19 Å for Cl−O. These values are in good agreement with experimental data,[41−43] namely, $r_{max} \cong 2.3$ Å first peak and $r_{max} \cong 3.7$ Å second peak for Cl−H; $r_{max} \cong 2.4$ Å for Na−O, and $r_{max} \cong 3.2$ Å for Cl−O.

The water coordination numbers around the Na and Cl ions can be estimated by integrating the area under the first peak of the Na−O and Cl−O pair distribution functions up to the first minimum, respectively. These coordination numbers are shown in Table 6 and give a good agreement with the experiments.

In addition to the thermodynamic functions already tested, it is important to validate our model with dynamic properties. Then, the shear viscosity, η, of the NaCl molecules immersed in

Table 6. Ion−Water Coordination Numbers Obtained by Our Simulations and Experiments[a]

molal concentration	MD NaO	MD ClO	exptl[44] NaO	exptl[44] ClO
2.4	4.75	6.55	4.83 (0.9)	6.68 (1.1)
4.05	4.55	6.4	4.55 (1.4)	6.5 (1.3)
6.1	4	6.15		

[a]The uncertainties of experimental data[44] are reported within parentheses, along with the r-range used in the integration.

water at different molal concentrations, at 289 K and at 1 bar, was evaluated. Figure 9 illustrates the viscosity versus molal concentration of the salt showing an increase of η as the salt concentration increases. This suggests that the addition of salt makes the system more viscous. Our result is consistent with the experimental values[5] and shows better agreement with the experiments when compared with the JJ[40] model in the TIP4P/ϵ and in the TIP4P water models, respectively. The figure also compares our findings with the JC$_{T4}$[32] model in the TIP4P/Ew water (light green triangles) and in the TIP4P/ϵ water, respectively (dark green triangles), indicating that the NaCl/ϵ shows a better performance.

Another important aspect of the dynamics of the particles is the diffusion. In this particular case it is interesting to observe how the water and the two ions change their mobilities with an increase in the salt concentration. This analysis can provide a good picture of the hydration process.

In Figure 10 the self-diffusion coefficient of water was measured for various salt concentrations at the temperature of 298 K and at 1 bar of pressure. The filled black diamond in this figure shows the experimental data,[5] and the blue filled diamonds are the results for our model. The purple and the dark blue triangles in Figure 10 are the results for the JJ[40] model in the TIP4P/ϵ and in the TIP4P water models, respectively. The light and dark green triangles in the same figure are the results for the JC$_{T4}$[32] model in the TIP4P/Ew and in the TIP4P/ϵ water models, respectively. As the molal concentration of the salt increases, the mobility of water molecules decreases. This behavior is consistent with the idea that, as the concentration of salt increases, there are fewer particles of water free. The water molecules are hydrating the ions, which slows down the dynamics of water. This result is in agreement with the increase of the viscosity illustrated in Figure 9.
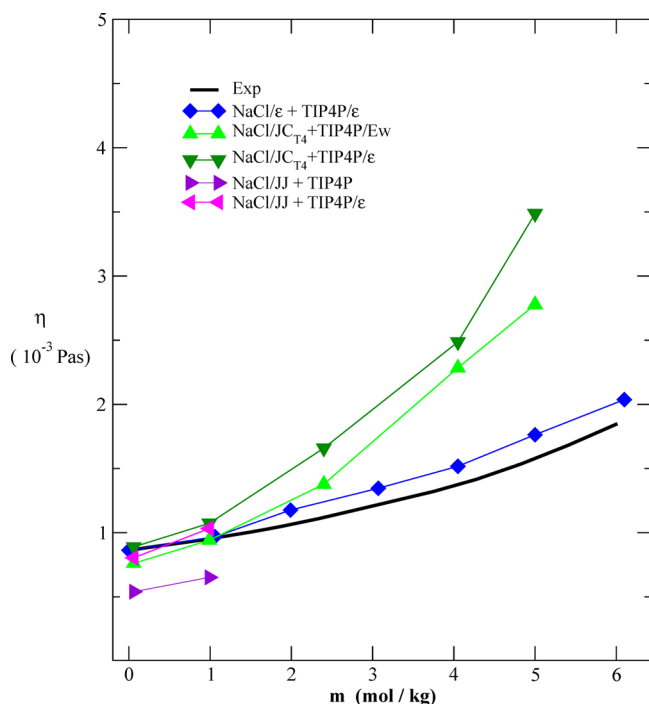
Figure 9. Viscosity of the NaCl molecules immersed in water versus molal concentration of the salt at the temperature of 298 K and at 1 bar of pressure. The black line is the experimental data,[5] and the blue filled diamonds are the results for the NaCl/ϵ model. The purple and the dark blue triangles are for the JJ model in the TIP4P/ϵ and in the TIP4P water models, respectively. The light and dark green triangles are the results for the JC$_{T4}$ model in the TIP4P/Ew and in the TIP4P/ϵ water models, respectively. All the simulations have been performed in this work.
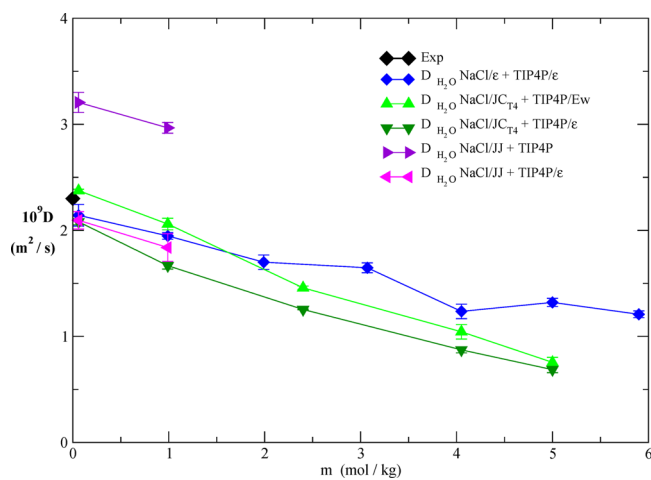

Figure 10. Diffusion coefficient of the water versus molal concentration of the salt at the temperature of 298 K and at 1 bar of pressure. The filled black diamond is the experimental data,[6] and the blue filled diamonds are the results for our model. The purple and the dark blue triangles are for the JJ model in the TIP4P/ϵ and in the TIP4P water models, respectively. The light and dark green triangles are the results for the JC$_{T4}$ model in the TIP4P/Ew and in the TIP4P/ϵ water models, respectively. All the simulations have been performed in this work.

The diffusion coefficient of the chloride ions versus molal concentration of the salt at the temperature of 298 K and at 1 bar of pressure is shown in Figure 11. The black line in this
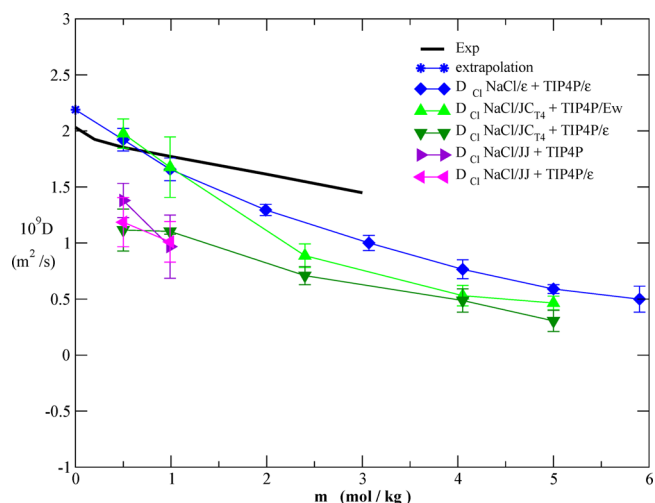

Figure 11. Diffusion coefficient of chloride versus molal concentration of the salt at the temperature of 298 K and at 1 bar of pressure. The black line is the experimental data,[6] and the blue filled diamonds are the results for the NaCl/ϵ model. The purple and the dark blue triangles are for the JJ model in the TIP4P/ϵ and in the TIP4P water models, respectively. The light and dark green triangles are the results for the JC$_{T4}$ model in the TIP4P/Ew and in the TIP4P/ϵ water models, respectively. All the simulations have been performed in this work.

figure indicates the experimental data,[5] and the blue filled diamonds are the results for our model. The purple and the dark blue triangles in Figure 11 are the results for the JJ[40] model in the TIP4P/ϵ and in the TIP4P water models, respectively. The light and dark green triangles in the same figure are the results for the JC$_{T4}$[32] model in the TIP4P/Ew and in the TIP4P/ϵ water models, respectively. The experimental data at infinite dilution of diffusion coefficient is $D_{Cl} = 2.032 \times 10^{-5}$ cm^2 s^{-1}. The system shows a decrease in mobility with the increase of the concentration which is the natural behavior of any molecular system. The increase of the number of particles decreases the mobility.

The diffusion coefficient of the sodium versus the molal concentration of the salt is shown in Figure 12. The black line in this figure illustrates the experimental data,[5] and the blue filled diamonds are the results for our model. The purple and the dark blue triangles in the same figure are the results for the JJ model in the TIP4P/ϵ and in the TIP4P water models, respectively. The light and dark green triangles in the Figure 12 are the results for the JC$_{T4}$ model in the TIP4P/Ew and in the TIP4P/ϵ water models, respectively. The diffusion coefficient of the sodium is almost constant when the salt concentration is increased. This behavior might be attributed to the small size of the hydrated sodium when compared with that of the hydrated chloride.

The solubility was computed employing method number four from the reference by Manzanilla-Granados et al.[27] as follows. At the beginning of the simulation, a nanocrystal is dipped into a 6.5 mol kg^{-1} solution of NaCl/ϵ ions and Tip4p/ϵ water. Values for the solubility were computed for a time up to 2 μs, as shown in Figure 13, which indicates that after 0.4 μs the simulation stabilizes with a fluctuation of 2.7%.

The solubility for the NaCl/ϵ is compared in Figure 14 with the experimental results and with the results for other models, showing that our model has better agreement with the experiments than the other models.
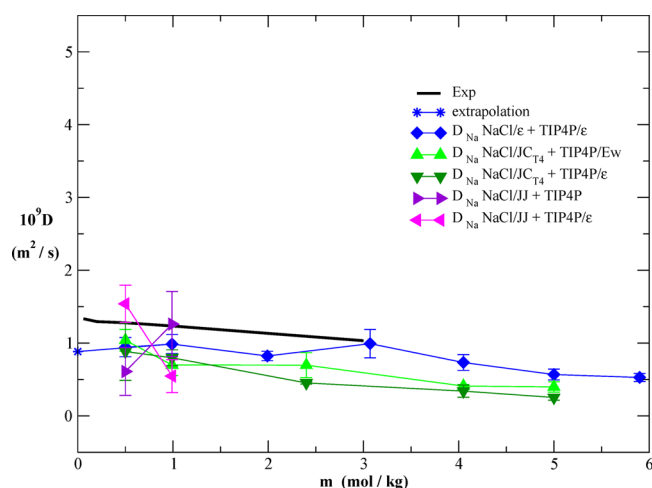
Figure 12. Diffusion coefficient of Na versus the molal concentration of the salt at temperature of 298 K and at 1 bar of pressure. The black line is the experimental data,[6] and the blue filled diamonds are the results for the NaCl/ϵ model. The purple and the dark blue triangles are for the JJ model in the TIP4P/ϵ and in the TIP4P water models, respectively. The light and dark green triangles are the results for the JC$_{T4}$ model in the TIP4P/Ew and in the TIP4P/ϵ water models, respectively. All the simulations have been performed in this work.
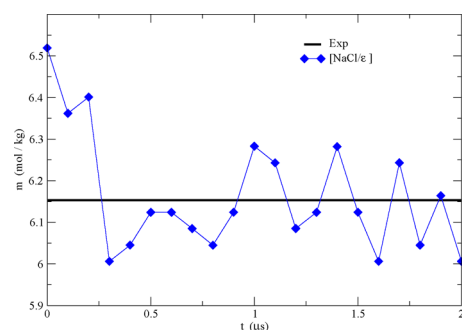

Figure 13. Solubility for the system NaCl/ϵ salt and Tip4p/ϵ water at 1 bar and 298 K.
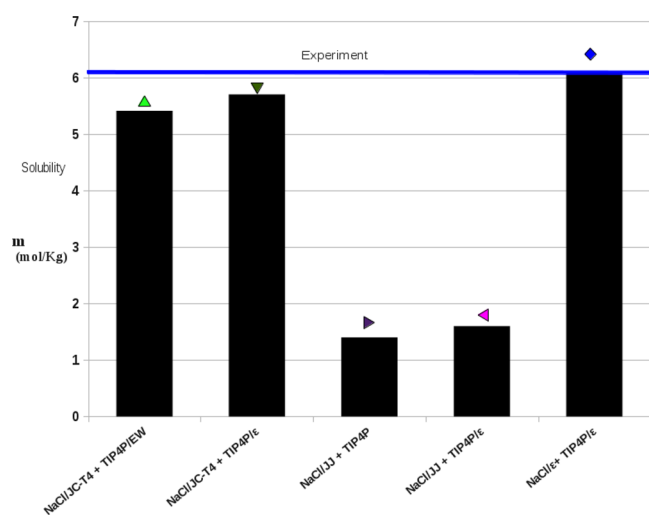

Figure 14. Solubility for 1 bar of pressure and 298 K of temperature for the following: the NaCl/ϵ salt in the TIP4P/ϵ water, for the JC$_{T4}$ salt in the TIP4P/Ew water and in the TIP4P/ϵ water, and JJ salt in the TIP4P/ϵ and in the TIP4P water. Experimental results are shown as the blue line.[5]

NaCl/ϵ in the SPC/ϵ Water. In order to further validate our model, we analyze the behavior of the NaCl/ϵ in a solution with a different water model. For this purpose the SPC/ϵ was selected. This force field reproduces very well the experimental dielectric constant and the density of pure water at various thermodynamic states. It fails, however, to reproduce the transport properties.[28]

First, Figure 15 shows the dielectric constant at 1 bar of pressure and at the temperature of 298 K for different molal
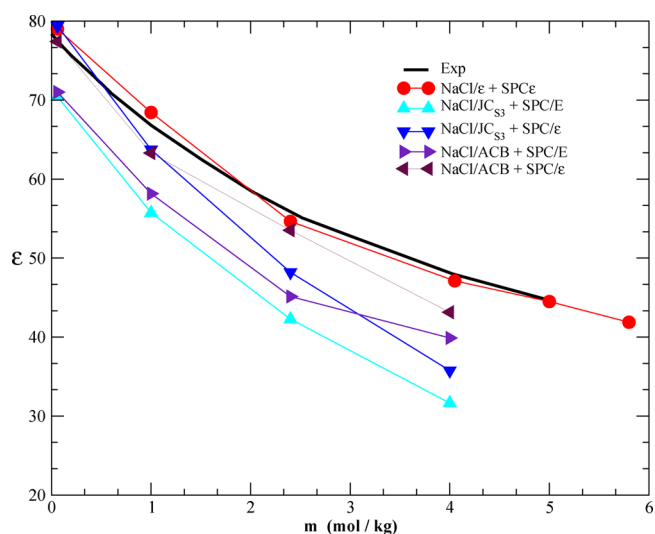

Figure 15. Dielectric constant versus molal concentration of salt at temperature of 298 K and 1 bar of pressure for the NaCl/ϵ model in the SPC/ϵ model for water (red circles), for the experiments[5] (solid black line), for the ACB[38] model in the SPC/E water (dark blue triangles) and in the SPC/ϵ water (black triangles), and for the JC$_{S3}$[32] model in the SPC/E water (light blue triangles) and in the SPC/ϵ water (blue triangles).

concentrations of salt for the NaCl/ϵ model in the SPC/ϵ model for water (red circles), for the experiments[5] (solid black line), for the ACB[38] model in the SPC/E water (dark blue triangles) and in the SPC/ϵ water (black triangles), and for the JC$_{S3}$[32] model in the SPC/E water (light blue triangles) and in the SPC/ϵ water (blue triangles). The graph shows that ϵ decreases as the concentration of salt increases due to the hydration effects as would be expected.

Next, the density was computed for different molal concentrations of the salt. Figure 16 illustrates the density for the NaCl/ϵ model in the SPC/ϵ model for water (red circles), for the experiments[5] (solid black line), for the ACB[38] model in the SPC/E water (dark blue triangles) and in the SPC/ϵ water (black triangles), and for the JC$_{S3}$[32] model in the SPC/E water (light blue triangles) and in the SPC/ϵ water (blue triangles). The NaCl/ϵ model in the SPC/ϵ underestimates the density. This might be due to the fact that the SPC/ϵ water model has a higher dipole moment when compared with that of the TIP4P/ϵ model.

Then, we also test the dynamics of the system. Figure 17 shows the viscosity, η, versus the molal salt concentration at 1 bar of pressure and 298 K of temperature of for the NaCl/ϵ model (red circles), for the experiments[5] (solid black line), for the ACB[38] model in SPC/E water (dark blue triangles) and in SPC/ϵ water (black triangles), and for the JC$_{S3}$[32] model in SPC/E water (light blue triangles) and in SPC/ϵ water (blue triangles).
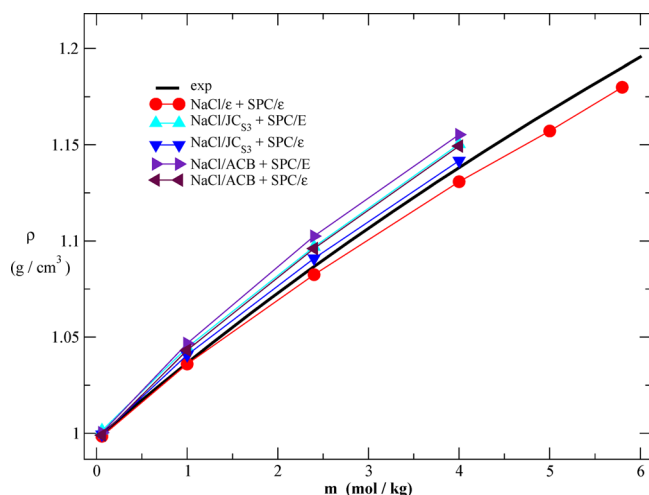
Figure 16. Density versus molal concentration of the salt at temperature of 298 K and 1 bar of pressure for the NaCl/ϵ model (red circles), for the experiments[5] (solid black line), for the ACB[38] model in SPC/E water (dark blue triangles) and in SPC/ϵ water (black triangles), and for the JC$_{S3}$[32] model in SPC/E water (light blue triangles) and in SPC/ϵ water (blue triangles).
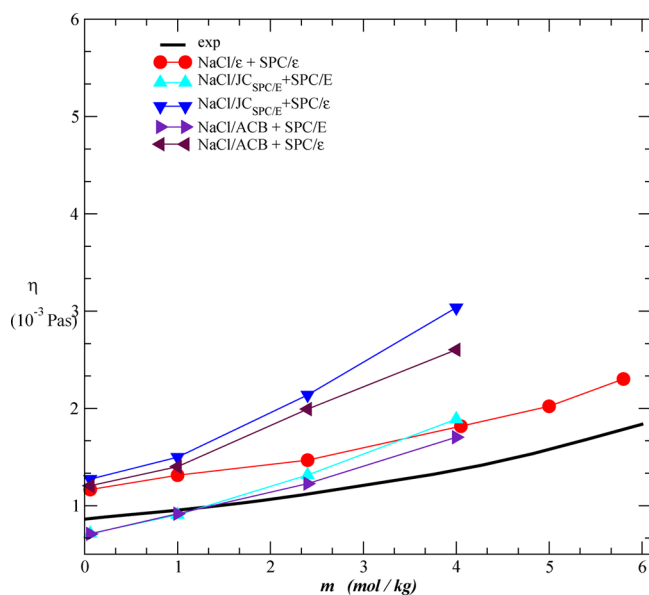

Figure 17. Shear viscosity versus molal concentration of salt at temperature of 298 K and 1 bar of pressure for the NaCl/ϵ model (red circles), for the experiments[5] (solid black line), for the ACB[38] model in SPC/E water (dark blue triangles) and in SPC/ϵ water (black triangles), and for the JC$_{S3}$[32] model in SPC/E water (light blue triangles) and in SPC/ϵ water (blue triangles).

The figure shows that the viscosity increases with the increase of the salt concentration which can be attributed to the solvation. The values for our model in the SPC/ϵ water show a shift in the solubility when compared with the experimental results. The origin of this shift is probably related to the fact that the SPC/ϵ does not perform well for dynamic properties. The constant shift therefore might be due to the constant concentration of water present in the solution.

In order to test if the incorrect dynamical behavior of the NaCl/ϵ and SPC/ϵ mixture is due to the problems in the water model, the diffusion coefficient is also computed. Figure 18 illustrates the diffusion coefficient of water versus the molal
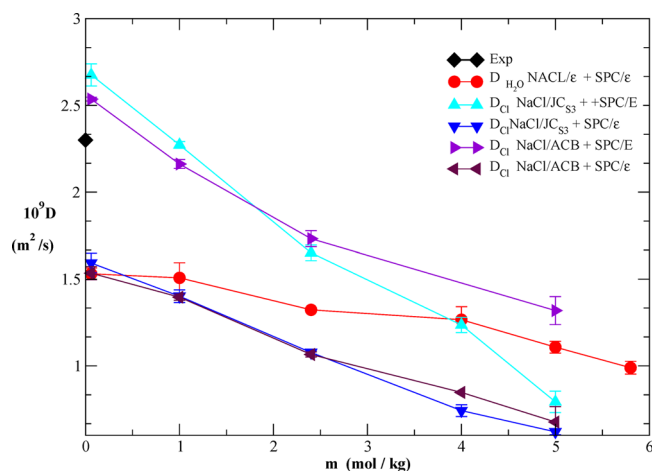

Figure 18. Diffusion coefficient of water versus molal concentration of the salt at temperature of 298 K and 1 bar of pressure for the NaCl/ϵ model (red circles), for the experiments[6] (black diamond), for the ACB[38] model in SPC/E water (dark blue triangles) and in SPC/ϵ water (black triangles), and for the JC$_{S3}$[32] model in SPC/E water (light blue triangles) and in SPC/ϵ water (blue triangles).

concentration of the salt at room pressure and temperature. D decreases with the increasing concentration of salt due to the solvation effects. The mobility for the NaCl/ϵ and SPC/ϵ mixture for low concentrations of salt is much lower than the diffusion coefficient observed for the NaCl/ϵ and TIP4P/ϵ water model and far below the experimental results.

The diffusion coefficient of the chloride is shown in Figure 19 at temperature of 298 K and 1 bar of pressure for the NaCl/
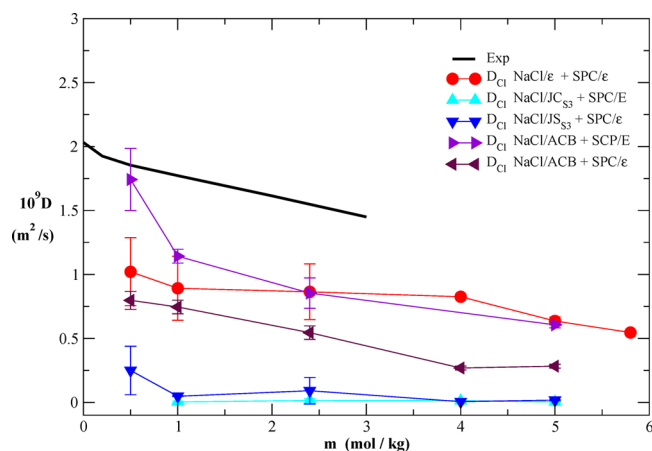

Figure 19. Diffusion coefficient of Cl versus molal concentration of the salt at temperature of 298 K and 1 bar of pressure for the NaCl/ϵ model (red circles), for the experiments[6] (black solid line), for the ACB[38] model in SPC/E water (dark blue triangles) and in SPC/ϵ water (black triangles), and for the JC$_{S3}$[32] model in SPC/E water (light blue triangles) and in SPC/ϵ water (blue triangles).

ϵ model (red circles), for the experiments[6] (black diamond), for the ACB[38] model in SPC/E water (dark blue triangles) and in SPC/ϵ water (black triangles), and for the JC$_{S3}$[32] model in SPC/E water (light blue triangles) and in SPC/ϵ water (blue triangles). It shows a smooth decrease with the concentration of salt.

Figure 20 shows the diffusion coefficient for the sodium versus the salt concentration at temperature of 298 K and 1 bar
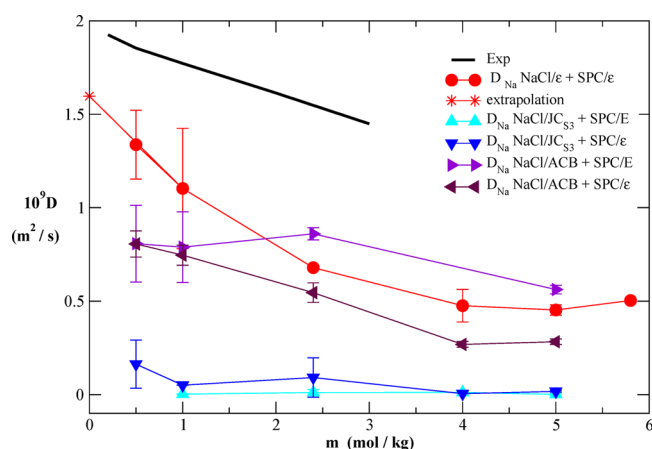
I

Figure 20. Diffusion coefficient of Na versus molal concentration of the salt at temperature of 298 K and 1 bar of pressure for the NaCl/ϵ model (red circles), for the experiments[6] (black solid line), for the ACB[38] model in SPC/E water (dark blue triangles) and in SPC/ϵ water (black triangles), and for the JC$_{S3}$[32] model in SPC/E water (light blue triangles) and in SPC/ϵ water (blue triangles).

of pressure for the NaCl/ϵ model (red circles), for the experiments[6] (black diamond), for the ACB[38] model in SPC/E water (dark blue triangles) and in SPC/ϵ water (black triangles), and for the JC$_{S3}$[32] model in SPC/E water (light blue triangles) and in SPC/ϵ water (blue triangles).

Finally, the solubility was also computed. The value obtained for the solubility for the NaCl/ϵ model in the SPC/ϵ water is 5.8 mol kg^{-1} with error ±0.15 mol kg^{-1} after 1 μs of simulation. The other values for SPC/ϵ were calculated in this work, and the others are taken from the original work.[26] The error bar is due to approximations in the method employed to calculate the solubility.[27] The NaCl/ϵ model in the SPC/ϵ water is compared with experiments and with other salt models in Figure 21, showing that it underestimates the value of the solubility when compared with the result for the solubility obtained with the NaCl/ϵ model in the TIP4P/ϵ water.

5. CONCLUSIONS

In this paper, we have proposed the NaCl/ϵ nonpolarizable model for NaCl. Within our approach the interaction potential of the ions combines a Lennard-Jones term and a Coulombic potential. The combination of the two terms is balanced by a parameter λ_i for each particle. The parametrization of our model uses experimental results for both the pure salt system and the mixture between the salt and water. In this process the water model selected for the salt−water mixture, the TIP4P/ϵ water model, shows the appropriated dielectric constant.

Then NaCl/ϵ model was validated by computing the density, the dielectric constant, the surface tension, the diffusion, and the viscosity for various concentrations of the salt. Our results for the pure salt system show a good agreement with the experiments, particularly when compared with the same quantities computed for other salt models.

In addition, the mixture of the NaCl/ϵ model with the TIP4P/ϵ water model was studied. The density, dielectric constant, diffusion, solubility, and viscosity were computed, showing a good agreement with experiments when compared with the results obtained using other salt and water models.

Finally, the NaCl/ϵ and SPC/ϵ mixture was analyzed. In this case, the thermodynamic quantities perform well, while the
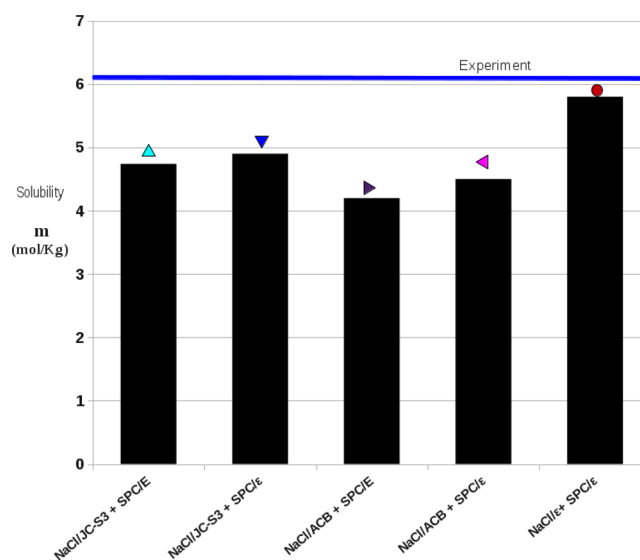

Figure 21. Calculus of the solubility using the direct coexistence method DCM, described by Manzanilla et al.,[27] at temperature of 298 K and 1 bar of pressure, for the NaCl/ϵ and SPC/ϵ. The other values for SPC/ϵ were calculated in this work, and the others are taken from the original work.[26] The blue line is the experimental data.[5]

diffusion shows discrepancies that in fact are consistent with the discrepancies of the bulk diffusion coefficient for this model. Our results indicate that the combination of the NaCl/ϵ with the TIP4P/ϵ models is good for describing salt solutions.

■ AUTHOR INFORMATION

Corresponding Authors
*E-mail: razcatl@hotmail.com.
*E-mail: marcia.barbosa@ufrgs.br.
Notes
The authors declare no competing financial interest.

■ REFERENCES

(1) Manning, G. S. The Molecular Theory of Polyelectrolyte Solutions with Applications to the Electrostatic Properties of Polynucleotides. *Q. Rev. Biophys.* **1978**, *11*, 179−246.

(2) Auffinger, P.; Bielecki, L.; Westhof, E. Anion Binding to Nucleic Acids. *Structure* **2004**, *12*, 379−388.

(3) Klein, D.; Moore, P.; Steitz, T. The Contribution of Metal Ions to the Structural Stability of the Large Ribosomal Subunit. *RNA* **2004**, *10*, 1366−1379.

(4) Hovland, M.; Kuznetsova, T.; Rueslåtten, H.; Kvamme, B.; Johnsen, H. K.; Fladmark, G. E.; Hebach, A. Sub-surface Precipitation of Salts in Supercritical Seawater. *Basin Research.* **2006**, *18*, 221−230.

(5) Lide, D. R. *CRC Handbook of Chemistry and Physics*, 90th ed.; CRC Press: Cleveland, OH, 2009.

(6) Kumamoto, E.; Kimizuka, H. Nonequilibrium Thermodynamics of Ionic Diffusion Coefficients in Binary Electrolyte Solutions. *Bull. Chem. Soc. Jpn.* **1979**, *52*, 2145−2146.

(7) Debye, P. W.; Hückel, E. The Theory of Electrolytes. I. Lowering of Freezing Point and Related Phenomena. *Physikalische Zeitschrift* **1923**, *24*, 185−206.

(8) Hoye, J. S.; Lebowitz, J. L.; Stell, G. Generalized Mean Spherical Approximations for Polar and Ionic Fluids. *J. Chem. Phys.* **1974**, *61*, 3253−3260.

(9) Essmann, U.; Perera, L.; Berkowitz, M. L.; Darden, T.; Lee, H.; Pedersen, L. G. A Smooth Particle Mesh Ewald Method. *J. Chem. Phys.* **1995**, *103*, 8577−8593.

(10) Allen, M. P.; Tildesley, D. J. *Computer Simulation of Liquids*; Oxford University Press: Oxford, U.K., 1987.

(11) Moučka, F.; Nezbeda, I.; Smith, W. R. Molecular Force Fields for Aqueous Electrolytes: SPC/E-Compatible Charged LJ Sphere Models and Their Limitations. *J. Chem. Phys.* **2013**, *138*, 154102−154111.

(12) Berendsen, H. J. C.; Postma, J. P. M.; van Gunsteren, W. F.; Hermans, J. Interaction Models for Water in Relation to Protein Hydration. *Intermolecular Forces*; Pullman, B., Ed.; Reidel: Dordrecht, 1981; pp 331−342.

(13) Berendsen, H. J. C.; Grigera, J. R.; Straatsma, T. P. The Missing Term in Effective Pair Potentials. *J. Phys. Chem.* **1987**, *91*, 6269−6271.

(14) Jorgensen, W. L.; Chandrasekhar, J.; Madura, J. D.; Impey, R. W.; Klein, M. L. Comparison of Simple Potential Functions for Simulating Liquid Water. *J. Chem. Phys.* **1983**, *79*, 926−934.

(15) Abascal, J. L.; Vega, C. A General Purpose Model for the Condensed Phases of Water: TIP4P/2005. *J. Chem. Phys.* **2005**, *123*, 234505−234517.

(16) Vega, C.; Abascal, J. L. Simulating Water With Rigid Non-Polarizable Models: A General Perspective. *Phys. Chem. Chem. Phys.* **2011**, *13*, 19663−19688.

(17) Fuentes-Azcatl, R.; Alejandre, J. Non-Polarizable Force Field of Water Based on the Dielectric Constant: TIP4P/ϵ. *J. Phys. Chem. B* **2014**, *118*, 1263−1272.

(18) Ferrario, M.; Ciccotti, G.; Spohr, E.; Cartailler, T.; Turq, P. Solubility of KF in Water by Molecular Dynamics Using the Kirkwood Integration Method. *J. Chem. Phys.* **2002**, *117*, 4947−4953.

(19) Sanz, E.; Vega, C. Solubility of KF and NaCl in Water by Molecular Simulation. *J. Chem. Phys.* **2007**, *126*, 014507−014520.

(20) Frenkel, D.; Ladd, A. J. C. New Monte Carlo Method to Compute the Free Energy of Arbitrary Solids. Application to the FCC and HCP Phases of Hard Spheres. *J. Chem. Phys.* **1984**, *81*, 3188−3193.

(21) Moučka, F.; Lísal, M.; Škvor, J.; Jirsák, J.; Nezbeda, I.; Smith, W. R. Molecular Simulation of Aqueous Electrolyte Solubility. 2. Osmotic Ensemble Monte Carlo Methodology for Free Energy and Solubility Calculations and Application to NaCl. *J. Phys. Chem. B* **2011**, *115*, 7849−7861.

(22) Moučka, F.; Lísal, M.; Smith, W. R. Molecular Simulation of Aqueous Electrolyte Solubility. 3. Alkali-Halide Salts and Their Mixtures in Water and in Hydrochloric Acid. *J. Phys. Chem. B* **2012**, *116*, 5468−5478.

(23) Lísal, M.; Smith, W. R.; Kolafa, J. Molecular Simulations of Aqueous Electrolyte Solubility: 1. The Expanded-Ensemble Osmotic Molecular Dynamics Method for the Solution Phase. *J. Phys. Chem. B* **2005**, *109*, 12956−12965.

(24) Orozco, G. A.; Moultos, O. A.; Jiang, H.; Economou, I. G.; Panagiotopoulos, A. Z. Molecular Simulation of Thermodynamic and Transport Properties for the H2O + NaCl System. *J. Chem. Phys.* **2014**, *141*, 234507−234511.

(25) Corradini, D.; Rovere, M.; Gallo, P. A Route to Explain Water Anomalies from Results on an Aqueous Solution of Salt. *J. Chem. Phys.* **2010**, *132*, 134508−134512.

(26) Joung, I. S.; Cheatham, T. E., III Molecular Dynamics Simulations of the Dynamic and Energetic Properties of Alkali and Halide Ions Using Water-Model-Specific Ion Parameters. *J. Phys. Chem. B* **2009**, *113*, 13279−13290.

(27) Manzanilla-Granados, H.; Saint-Martin, H.; Fuentes-Azcatl, R.; Alejandre, J. Direct Coexistence Methods to Determine the Solubility of Salts in Water from Numerical Simulations. Test Case NaCl. *J. Phys. Chem. B* **2015**, *119*, 8389−8396.

(28) Fuentes-Azcatl, R.; Mendoza, N.; Alejandre, J. Improved SPC Force Field of Water Based on the Dielectric Constant: SPC/ϵ. *Phys. A* **2015**, *420*, 116−123.

(29) Hansen, J. P.; McDonald, I. R. *Theory of Simple Liquids*; 3rd ed.; Academic: Amsterdam, The Netherlands, 2006.

(30) Smith, D. E.; Dang, L. X. Computer simulations of NaCl Association in Polarizable Water. *J. Chem. Phys.* **1994**, *100*, 3757−3766.

(31) Leontyev, I. V.; Stuchebrukhov, A. A. Polarizable Molecular Interactions in Condensed Phase and Their Equivalent Nonpolarizable Models. *J. Chem. Phys.* **2014**, *141*, 014103−014115.

(32) Joung, I. S.; Cheatham, T. E., III Determination of Alkali and Halide Monovalent Ion Parameters for Use in Explicitly Solvated Biomolecular Simulations. *J. Phys. Chem. B* **2008**, *112*, 9020−9041.

(33) Hess, B.; Kutzner, C.; van der Spoel, D.; Lindahl, E. GROMACS 4: Algorithms for Highly Efficient, Load-Balanced, and Scalable Molecular Simulation. *J. Chem. Theory Comput.* **2008**, *4*, 435−447.

(34) Essmann, U.; Perera, L.; Berkowitz, M. L.; Darden, T.; Lee, H.; Pedersen, L. G. A Smooth Particle Mesh Ewald Method. *J. Chem. Phys.* **1995**, *103*, 8577−8593.

(35) Hess, B.; Bekker, H.; Berendsen, H. J. C.; Fraaije, J. G. E. M. LINCS: A Linear Constraint Solver For Molecular Simulations. *J. Comput. Chem.* **1997**, *18*, 1463−1472.

(36) Tuckerman, M. E.; Liu, Y.; Ciccotti, G.; Martyna, G. J. Non-Hamiltonian Molecular Dynamics: Generalizing Hamiltonian Phase Space Principles to Non-Hamiltonian Systems. *J. Chem. Phys.* **2001**, *115*, 1678−1702.

(37) Alejandre, J.; Tildesley, D. J.; Chapela, G. A. Molecular Dynamics Simulation of the Orthobaric Densities and Surface Tension of Water. *J. Chem. Phys.* **1995**, *102*, 4574−4583.

(38) Alejandre, J.; Chapela, G. A.; Bresme, F.; Hansen, J. P. the Short Range Anion-H Interaction is the Driving Force for Crystal Formation of Ions in Water. *J. Chem. Phys.* **2009**, *130*, 174505−174515.

(39) Neumann, M. Dipole Moment Fluctuation Formulas in Computer Simulations of Polar Systems. *Mol. Phys.* **1983**, *50*, 841−858.

(40) Jensen, K. P.; Jorgensen, W. L. Halide, Ammonium, and Alkali Metal Ion Parameters for Modeling Aqueous Solutions. *J. Chem. Theory Comput.* **2006**, *2*, 1499−1509.

(41) De-Jong, P. H. K.; Neilson, G. W.; Bellissent-Funel, M. C. Hydration of Ni^{2+} and Cl$^-$ in a Concentrated Nickel Chloride Solution at 100°C and 300°C. *J. Chem. Phys.* **1996**, *105*, 5155−5162.

(42) Powell, D. H.; Neilson, G. W.; Enderby, J. E. The Structure of Cl$^-$ in Aqueous Solution: an Experimental Determination of g$_{ClH}$(r) and g$_{ClO}$(r). *J. Phys.: Condens. Matter* **1993**, *5*, 5723−5730.

(43) Skipper, N. T.; Neilson, G. W. X-ray and Neutron Diffraction Studies on Concentrated Aqueous Solutions of Sodium Nitrate and Silver Nitrate. *J. Phys.: Condens. Matter* **1989**, *1*, 4141−4151.

(44) Mancinelli, R.; Botti, A.; Bruni, F.; Ricci, M. A.; Soper, A. K. Hydration of Sodium, Potassium, and Chloride Ions in Solution and the Concept of Structure Maker/Breaker. *J. Phys. Chem. B* **2007**, *111*, 13570−13577.

(45) Fernandez-Prini, P. International Association for the Properties of Water and Steam; http://www.iapws.org/relguide/IF97-Rev.pdf, 2007 (Accessed June 1, 2015).